

# New Intumescent Flame-Retardant Agent: Application to Polyurethane Coatings

Jincheng Wang, Guang Li,\* Shenglin Yang, Jianming Jiang

State Key Laboratory for Modification of Chemical Fibers and Polymer Materials, Donghua University, Shanghai, 200051, China

Received 18 July 2002; accepted 14 June 2003

**ABSTRACT:** The first part of this investigation focused on the synthesis and characterization of a new type of intumescent flame-retardant (IFR) agent. Four steps were used in the synthesis process. The structure was characterized by FTIR, magic-angle spinning nuclear magnetic resonance (MAS-NMR)  $^{13}\text{C}$  spectroscopy, and elemental analysis. The addition of an IFR agent into polyurethane (PU) varnish led to an improvement in its carbonization and flame-retardant (FR) properties. The second part focused on the evaluation of

such characteristics as FR property, thermal stability of IFR/PU-based coatings, rheology of IFR/PU-based coating solutions, and mechanical properties such as hardness, adhesion, and flexibility of IFR/PU-based dry coating films. © 2003 Wiley Periodicals, Inc. *J Appl Polym Sci* 91: 1193–1206, 2004

**Key words:** flame retardance; films; synthesis; coatings; polyurethanes

## INTRODUCTION

Polyurethane (PU) polymers have been developed into many types and classes of products with widely varying properties that result from the ingredients of the formulation. Foams, either flexible or rigid, are the most common commercial products. Moreover, PUs are also extensively used as resins for lacquers, varnishes, and coatings; composites in synthetic leather, adhesives, and spandex fibers; and they can be cast, injection molded, or extruded as elastomers.<sup>1–5</sup>

PU-based coatings have recently assumed an important place in the coatings industry. In some applications, they dominate the market because of their high level of quality.<sup>6</sup> First, they combine outstanding resistance to solvents and chemicals with good weather stability. Second, the films show excellent mechanical properties and provide the ideal balance of hardness and flexibility, even at low temperatures.

Like a majority of synthetics, PU-based coatings are combustible, which consequently limits their use in buildings or in transport applications. A practical approach to enhance its fire safety capability is the incorporation of flame-retardant (FR) additives in the PU polymeric matrix.<sup>7,8</sup> The use of intumescent additives allows both fire-related properties and mechanical behavior of the materials to be optimized. During

the heating process, an intumescent flame-retardant (IFR) agent generates a cellular charred layer on the surface of the material, which protects the underlying material from the action of the heat flux or flame and acts as a physical barrier that limits the diffusion of combustible volatile products toward the flame and of oxygen toward the polymer. The proposed mechanisms are based on the charred layer acting as a physical barrier, which slows down heat and mass transfer between the gas and condensed phases.<sup>9,10</sup>

An IFR system usually contains three main substances: an acid source, a carbon source, and a gas source. They are usually used as combinations and the typical example is the composite of ammonium–polyphosphate (APP), pentaerythritol (PER), and melamine (ME).<sup>11,12</sup>

Recently, a novel IFR additive, which contains the above three functional sources and shows IFR capabilities, was proposed.<sup>12</sup> However, the FR performance and the thermal stability of this compound are different according to different molecular structures. In our work, single compounds of differing structure were synthesized and added to PU-based coatings. First, this study reports on the synthesis and characterization of the new IFR agent. Then, the FR capabilities and thermal stability of the IFR/PU-based coatings, the rheology of IFR/PU-based coating solutions, and evaluation of the mechanical performances of a sandwich material (woodblocks + IFR/PU-based coating) are presented.

## EXPERIMENTAL

### Materials

To synthesize this new IFR agent, cyanuric chloride (industrial-grade; supplied by Liaoning Organic Plant,

\*Present address: College of Material Science and Engineering, Donghua University, Shanghai, 200051, China.

Correspondence to: G. Li (lig@dhu.edu.cn).

China), strong ammonia, anhydrous sodium carbonate, ethanolamine (analytically pure; supplied by Shanghai Chemical Reagent No. 1 Plant, China), PER, and phosphorus oxychloride ( $\text{POCl}_3$ , analytically pure; provided by Shanghai Chemical Reagent No. 2 Plant, China) were used. The surfactant, a silane coupling agent (KH570), was received from Shanghai Yaohua Organic Chemical Corp. (China). Bentonite was supplied by Shanghai Chemical Plant (China). To perform a systematic study of the influence of addition of an IFR agent on the FR and mechanical properties of PU-based coatings, a PU solvent-based varnish (two components; supplied by Shanghai Hua-shen Coating Corp., China) was prepared. The woodblocks used in FR tests were five-ply birch veneers bought from a local store in Shanghai.

The IFR agent was milled in an Airflow-Miller 855. The average size of the particles was about  $2.5 \mu\text{m}$  according to optical microscopy analysis. To avoid the precipitation of additives from the PU solutions, a silane coupling agent and bentonite were used. The IFR/PU solutions were prepared in the following two stages<sup>13</sup>:

1. The IFR agent, mixed with a small amount of silane coupling agent and bentonite, was stirred at 2500 rpm for 10 min in a laboratory mixer.
2. The mixture was added to the PU varnish. This mixture was stirred in the laboratory triturator at 12,000 rpm for 10 min; then the solution was ground by mortar (similar to ball-milling) for 20 min; finally, a homogeneous solution was obtained. This preparation procedure avoided precipitation of the IFR agent from the solution (monitored 1 month after preparing the solution).

The IFR/PU-based coatings were sprayed onto the woodblocks ( $30 \times 15 \times 0.6 \text{ cm}^3$ ). The testing woodblocks were kept in a controlled atmosphere of  $50 \pm 5\%$  relative humidity and  $23 \pm 2^\circ\text{C}$  for 14 days before coating. Before the burning tests, the specimens were kept in an oven at  $50 \pm 0.2^\circ\text{C}$  for a period of 2 h.

## Characterization

### FTIR spectroscopy

FTIR spectra were recorded on a Nicolet 170SX Fourier transform infrared spectrophotometer (Nicolet Analytical Instruments, Madison, WI) in the range  $4000\text{--}400 \text{ cm}^{-1}$  at a resolution of  $2 \text{ cm}^{-1}$ . Samples were ground and mixed with KBr to form pellets. Sixty-four scans were necessary to obtain spectra with good signal-to-noise ratios.

MAS-NMR  $^{13}\text{C}$  spectroscopy of the solid-state intermediate II and IFR agent

Solid-state magic-angle spinning nuclear magnetic resonance (MAS-NMR)  $^{13}\text{C}$  spectroscopy of interme-

diante II and the IFR agent was performed using a DSX300 spectrometer at a spinning speed of 300.13 MHz, with high-power  $^1\text{H}$  decoupling and  $^1\text{H}\text{--}^{13}\text{C}$  cross polarization (CP). The Hartmann-Hahn matching condition was obtained by adjusting the power on the  $^1\text{H}$  channel for a maximum  $^{13}\text{C}$  free-induction delay signal of adamantane. All spectra were acquired with contact times of 2 ms. The  $^{13}\text{C}$   $\pi/2$  pulse width was 4.1 ms. A repetition time of 5 s was used for all samples because the spin-lattice relaxation time ( $T_1$ ) remained below 1 s (the repetition time was chosen to be more than five times  $T_1$ ). Some 696 scans were necessary to obtain spectra with good signal-to-noise ratios, and the reference used was tetramethylsilane.

### Elemental analysis of intermediate II and IFR agent

Samples were examined by elemental analysis on a Heraeus CHN-0-Rapid analyzer. Determination of the amounts of carbon and hydrogen was made by burning the sample in an excess of oxygen at  $1000^\circ\text{C}$ . The quantity of the evolved  $\text{CO}_2$  was then determined by coulometry and was proportional to the total quantity of carbon in the sample. The quantity of nitrogen was determined by burning the sample in He with 3% oxygen at  $1000^\circ\text{C}$ . The evolved nitrogenated oxides were then reduced to molecular nitrogen, the quantity of which was determined with a catharometer.

### Rheology of IFR/PU-based coating solutions

The viscosity, pseudoplasticity, and thixotropy of filled PU coating solutions were analyzed using an NDJ-8S digital viscosity and rheometer. The measurements were carried out at  $20^\circ\text{C}$  in the rotational mode using a concentric cylinder, type Z3 (according to the viscosity of the system). A PU-based solution (100 mL) was used in the measurements and a solvent trap ensured that minimal evaporation of solvent occurred during the experiments. Controlled shear rate experiments were carried out as follows: the shear rate was increased to 0.3 rpm and maintained for 1 min to provide a uniform and standardized state in all the solutions.<sup>13</sup> The experiments were carried out by increasing, within 120 s, the shear rate to 60 rpm; this shear rate was maintained for 60 s and then was decreased to 0 rpm within 120 s. Some experiments were repeated and excellent reproducibility was always obtained.

### FR tests

The limiting oxygen index (LOI) was measured using a Stanton Redcroft instrument on sheets ( $100 \times 10 \times 3 \text{ mm}^3$ ) according to ASTM 2863.

Samples ( $100 \times 100 \times 10 \text{ mm}^3$ ) were exposed to a Stanton Redcroft Cone Calorimeter according to

ASTM 1356-90 under a heat flux of  $50 \text{ kW/m}^2$  (this external flux was chosen because it corresponds to the heat evolved during a well-developed fire).<sup>14,15</sup> Three tests were conducted on each material; medium results were extracted from these tests to limit uncertainties in the measurements.

The rate of heat release (RHR) represents the evolution of energy flow versus time for a given sample surface. The total heat evolved (THE) was obtained from the integration of the RHR curves. The equipment also allows for the determination of carbon monoxide (CO) and carbon dioxide (CO<sub>2</sub>) concentrations in the combustion gases.<sup>16</sup>

The flame retardancy of the IFR/PU-coated woodblocks was also evaluated by weight loss and char index according to GB/T 15442.3 (ASTM D1360-2000, cabinet method). The application rate of every coating was  $500 \text{ g/m}^2$ . The depth of coating films was about 0.6 mm (measured according to ASTM D 5235-97).

#### Photography and scanning electron microscopy (SEM)

Scanning photographs of the shape of different types of char were performed on an Epson Perfection 610 scanning instrument. SEM analysis of a typical char structure was carried out using a Comscan Series 4 instrument. The samples were gold coated using an IB-3 ionic sputtermeter.

#### Thermal analyses

Thermogravimetric analysis (TGA) was carried out at  $10^\circ\text{C}/\text{min}$  under air (flow rate  $5 \times 10^{-7} \text{ m}^3/\text{s}$ , air liquid grade) using a DuPont 1090 microbalance (DuPont, Boston, MA). In each case, the mass of the sample used was fixed at 10 mg and the samples (powder mixtures) were positioned in open vitreous silica pans. The precision of the temperature measurements was  $1^\circ\text{C}$  over the whole range of temperatures. The curves of weight differences between the experimental and theoretical TGA curves were computed as follows:

$M_{\text{PU}}(T)$ : values of weight given by TGA curve of PU

$M_{\text{IFR}}(T)$ : values of weight given by TGA curve of the IFR agent

$M_{\text{exp}}(T)$ : values of weight given by TGA curves of IFR agent/PU

$M_{\text{th}}(T)$ : TGA curves computed by linear combination between the values of weight given by TGA curves of PU and the additives:  $M_{\text{th}}(T) = 0.3M_{\text{IFR}}(T) + 0.7M_{\text{PU}}(T)$

$\Delta(T)$ : curve of weight difference;  $\Delta(T) = M_{\text{exp}}(T) - M_{\text{th}}(T)$

The  $\Delta(T)$  curves enabled observation of an eventual increase or decrease in the thermal stability of the

polymer related to the presence of the additives. The IFR ratio using the calculation of  $M_{\text{th}}(T)$  was determined as follows: first, 3 g of paint was weighed out into a flat-bottom dish and heated for about 3 h in an oven at  $105^\circ\text{C}$ ; Then, it was cooled, weighed, and reheated for a further 0.5 h to check that the weight was constant. The ratio of IFR/PU (20/80 wt %) was 3/7 (w/w) as a result of the volatilization of organic solvent.

#### Mechanical properties of dry IFR/PU-based coatings

##### Crosslinking level test

The IFR/PU coating solutions were coated onto a set of glass plates at  $23 \pm 2^\circ\text{C}$  for 72 h and then put in an oven at  $80^\circ\text{C}$  for 30 min. The films were then removed and immersed into PU special thinner for 24 h. The crosslinking level was determined from the ratio between the remaining and the initial weight of the polymer.<sup>17</sup>

##### Hardness test

The film hardness of coated-woodblocks was performed according to GB/T 6739-1996 (similar to ASTM D 3363-00). In this test, a set of calibrated drawing leads (preferred) or equivalent calibrated wood pencils meeting the following scale of hardness were used:

6B-5B-4B-3B-2B-B-HB-F-H-2H-3H-4H-5H-6H-7H-8H-9H (from softer to harder)

The depth of dry coating film was 0.6 mm. The test was conducted at  $23 \pm 2^\circ\text{C}$  and  $50 \pm 5\%$  relative humidity.

##### Adhesion test

Adhesion of the coatings to their substrates was measured by a crosscut tape test (GB 9286-88, similar to ASTM D 3359, Method A) tests. The coatings were inspected and evaluated according to the following 0 to 5 grading system:

- 0 No peel or removal of coating
- 1 Trace peeling or removal along the cuts
- 2 Jagged removal along cuts up to 1.6 mm on either side
- 3 Jagged removal along the majority of cuts up to 3.2 mm on either side
- 4 Removal from over 50% of the area under the tape
- 5 Removal of all the coating under the tape or beyond the tape

## FTIR Spectra

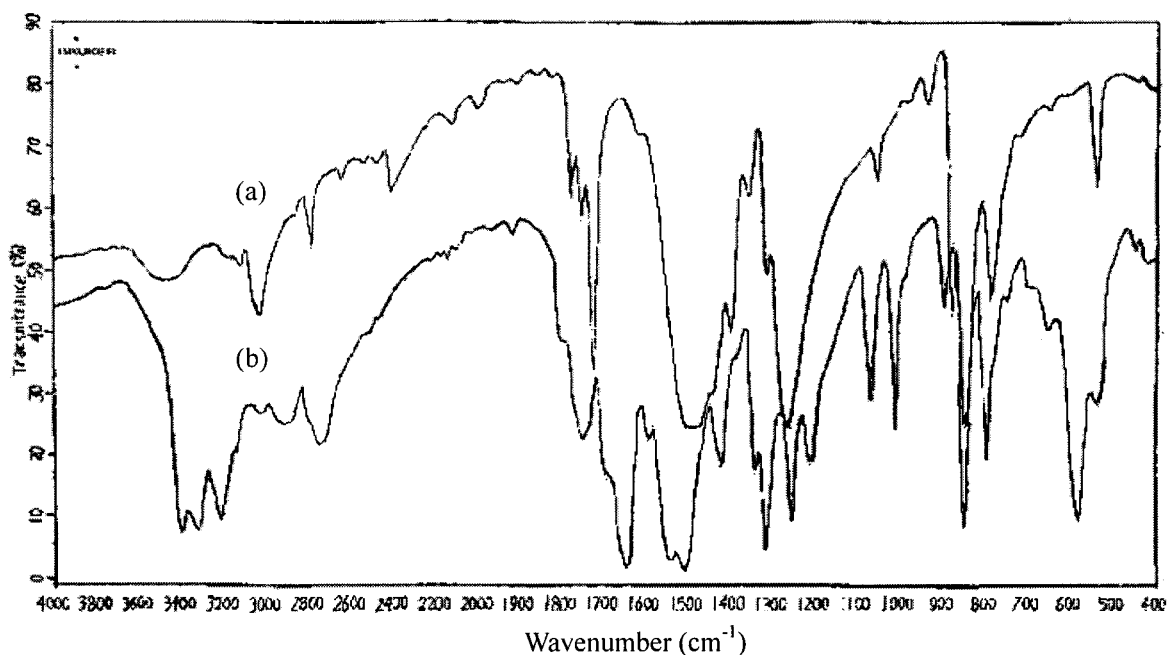


Figure 1 FTIR spectra of (a) cyanuric chloride and (b) intermediate I.

### Flexibility test

Flexibility of the coatings was evaluated according to GB/T 1731-93. In this test, the coating was applied to  $120 \times 2.5 \times 0.2$ -mm soft tin and allowed to harden for the specified time. The panel was then placed, coating side outermost, under a mandrel of prescribed diameter embodied in a hinge. The panel was bent through  $180^\circ$  in 1 s and removed, and the bend was examined for cracks and loss of adhesion. Mandrels in use ranged from 15 to 0.5 mm (15, 10, 5, 4, 1.5, 1, 0.5). The

minimum diameter through which the coating film cannot be damaged was used to represent its flexibility.

## RESULTS AND DISCUSSION

### Syntheses

#### Synthesis of intermediate I

Distilled water (100 mL) was prepared and added to a three-neck flask provided with a stirrer. The flask was

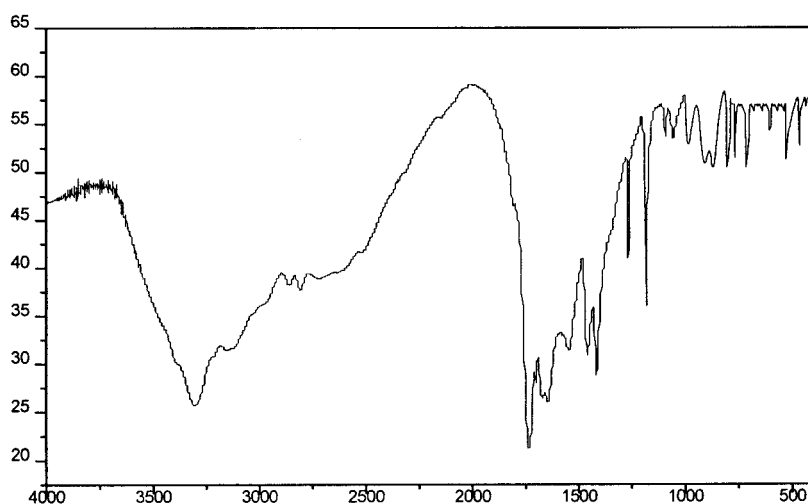


Figure 2 FTIR spectrum of intermediate II.

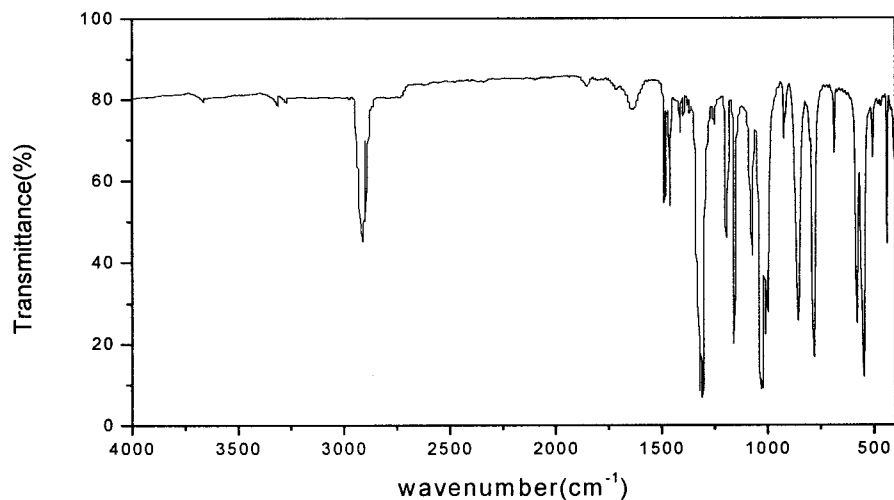


Figure 3 FTIR spectrum of intermediate III.

placed in a cold water bath, the temperature of which was kept at 0°C. A solution of 0.5 mol cyanuric chloride and 100 mL acetone was prepared. It was quickly added to the flask, with continuous stirring. Then 0.5 mol strong ammonia and 0.25 mol anhydrous sodium carbonate were added to the mixture with continuous stirring. After reaction at 0°C for about 1 h, the product was separated by filtration, washed, and dried in vacuum until achieving a constant weight. The product was obtained as a stable pale yellow powder (yield ~ 90%; m.p. ~ 240°C).

#### Synthesis of intermediate II

Distilled water (80 mL) was added to a three-neck flask. Intermediate (0.5 mol) I and ethanolamine (0.5 mol) were added to the flask. During the process of reaction, 0.5 mol anhydrous sodium carbonate was

added dropwise to the mixture and the mixture was kept neutral during the process of reaction. After stirring for about 2 h, the reaction was stopped. The product was purified by filtration, washed, and dried in vacuum.

The product was obtained as a white powder and its molecular weight was analyzed by end-group analysis (yield ~ 85%; m.p. ~ 300°C).

#### Synthesis of intermediate III

POCl<sub>3</sub> (250 mL) and PER (0.5 mol) were added to a three-neck flask and the reaction was carried out at 100°C for 24 h. Then, the product was separated by filtration, and after washing by methylene chloride, the product was dried in vacuum until achieving a constant weight. The product was obtained as a white powder (yield ~ 70%; m.p. ~ 242–245°C).

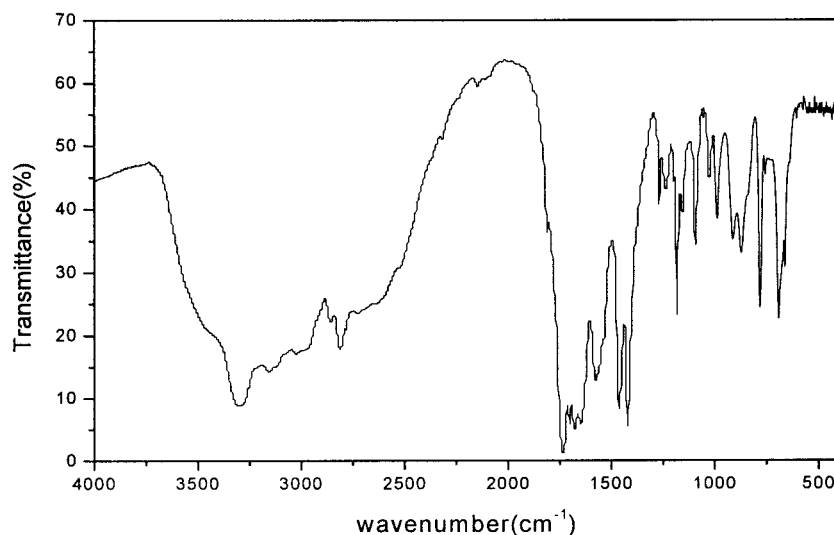
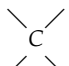
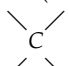


Figure 4 FTIR spectrum of the IFR agent.

TABLE I  
Assignment of Main FTIR Band Absorption in Raw Material,  
Intermediates, and IFR Agent

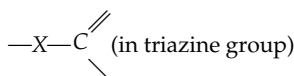
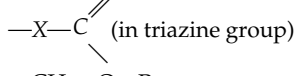
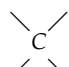
Material	Band position (cm <sup>-1</sup> )	Assignment	Refs.
Cyanuric Chloride	1500, 878, 848	Triazine	[18,19]
	536	$\nu$ C(triazine)—Cl	[20]
Intermediate I	3400, 3313	$\nu$ NH <sub>2</sub> (linked to triazine)	[18,21]
	1630	$\delta$ NH <sub>2</sub> (linked to triazine)	[18,21]
	563	$\nu$ C(triazine)—Cl	[20]
Intermediate II	1500, 886, 848	Triazine	[18]
	3450	$\nu$ NH (linked to triazine)	[20,21]
	1265	$\nu$ C(triazine)—O—C	[20,21]
	2808, 2850	$\nu$ —CH <sub>2</sub> —CH <sub>2</sub>	[20,21]
	1465	$\delta$ —CH <sub>2</sub> —CH <sub>2</sub>	[20,21]
	3350	$\nu$ NH <sub>2</sub> (linked to triazine)	[18,20,21]
Intermediate III	1500, 878, 848	Triazine	[18,21]
	2900	—CH <sub>2</sub>	[16,20]
	1280	—P=O	[16,20]
	1150		[16,20]
IFR agent	1032	—P—O—C	[16,20]
	980, 780, 690	Spirocyclic	[16,20]
	546	P—Cl	[16,20]
	3500	$\nu$ NH (linked to triazine)	[20]
	3300	$\nu$ NH <sub>2</sub> (linked to triazine)	[20]
	3000	$\nu$ NH <sub>3</sub> <sup>+</sup>	[16,20]
	1575	$\delta$ NH <sub>3</sub> <sup>+</sup>	[16,20]
	2800–2900	$\nu$ —CH <sub>2</sub> —CH <sub>2</sub>	[20]
	1390	$\delta$ —CH <sub>2</sub> —CH <sub>2</sub>	[20]
	1280	—P=O	[16,20]
	1240	$\nu$ C(triazine)—O—C	[16]
	1150		[16]
	1032	—P—O—C	[20]
1450, 878, 848	Triazine	[18]	

#### Synthesis of IFR agent

Intermediate III (0.5 mol) and intermediate II (0.5 mol) were added to a 500-mL three-neck flask. After stirring at 90°C for about 1.5–2 h, the product was cooled

and separated by water, after which it was dried in vacuum until reaching a constant weight. The product was obtained as a white powder (yield: ~ 80%; m.p. ~ 310°C).

TABLE II  
Assignment of MAS/NMR <sup>13</sup>C Chemical Shifts of IFR Agent

	Chemical shift (ppm)	Assignment	Refs.
Intermediate II	150–170	 (in triazine group)	[21,22]
	60	—O—CH <sub>2</sub> —	[21,22]
IFR agent	42	—NH—CH <sub>2</sub> —	[21,22]
	140–170	 (in triazine group)	[22]
	70	—CH <sub>2</sub> —O—P	[22]
	48	—O—CH <sub>2</sub> —	[22]
	60		[22]
	39	—NH—CH <sub>2</sub> —	[22]

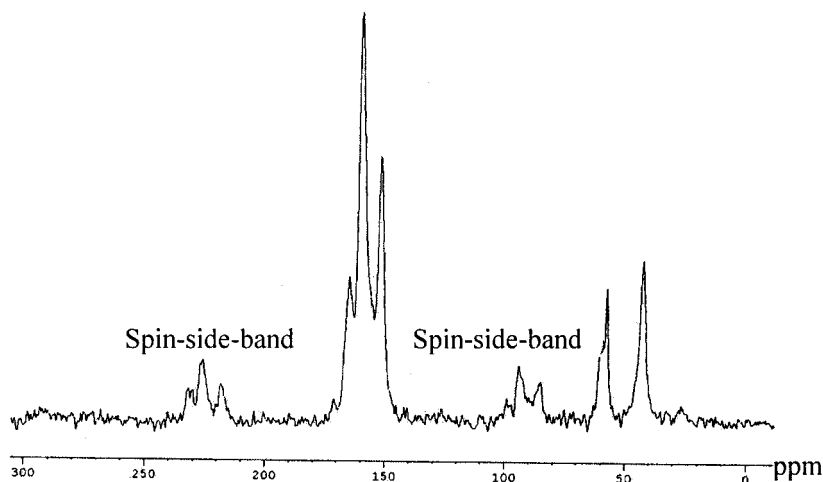


Figure 5 MAS-NMR  $^{13}\text{C}$  spectrum of intermediate II.

### Characterization

#### FTIR spectra

Figures 1, 2, 3, and 4 show the FTIR spectra of cyanuric chloride [Fig. 1(a)] and intermediate I [Fig. 1(b)]; intermediate II; intermediate III; and the IFR agent, respectively. Absorption data from all these spectra are summarized in Table I.

We can conclude from Table I that one C—Cl bond in cyanuric chloride was successfully replaced by one  $-\text{NH}_2$  group after reacting with strong ammonia, and the other two C—Cl bonds were substituted by  $-\text{O}-\text{CH}_2-\text{CH}_2$  and  $-\text{NH}-\text{CH}_2-\text{CH}_2$  when the second step was completed. Also, we confirmed that  $\text{POCl}_3$  reacts with PER and leaves only one  $-\text{Cl}$  bond that still has activity. The disappearance of absorp-

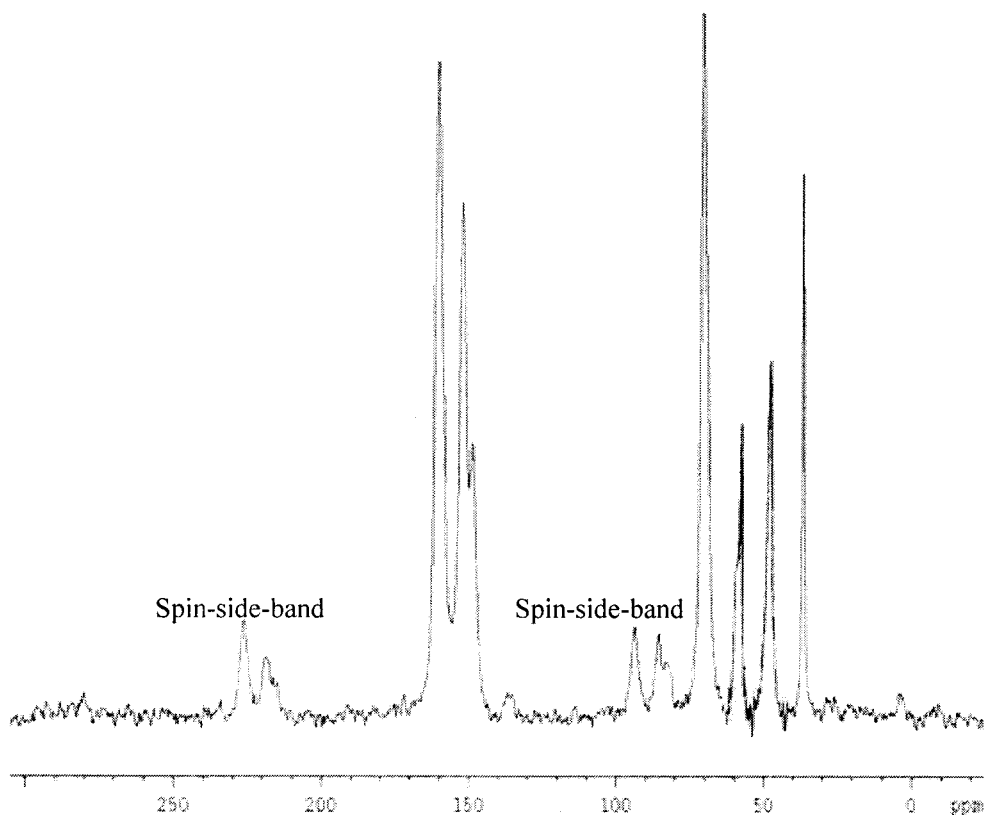


Figure 6 MAS-NMR  $^{13}\text{C}$  spectrum of the IFR agent.

tions around 500–600  $\text{cm}^{-1}$  in the FTIR spectrum of the final IFR agent indicates the thorough replacement of the Cl element in the structure.

#### MAS-NMR $^{13}\text{C}$ spectra of the solid-state intermediate II and IFR agent

The MAS-NMR  $^{13}\text{C}$  spectra of intermediate II and the IFR agent are shown in Figures 5 and 6, and their data are listed in Table II. In the two figures, three intense bands may be observed between 140 and 170 ppm that are assigned to the three carbons of the triazine group in the intermediate II and IFR agent attributed to the electron-withdrawing effect of the  $-\text{NH}_2$ ,  $-\text{O}-\text{CH}_2-\text{CH}_2$ , and  $-\text{NH}-\text{CH}_2-\text{CH}_2$  groups. In Figure 5, the chemical shifts at 42 and 60 ppm are attributed to the two carbons of the  $-\text{CH}_2-\text{CH}_2$  group in the intermediate. In Figure 6, the chemical shifts at 60 and 70 ppm may be assigned to the quarter carbon in the  $>\text{C}<$  structure and the carbon in the  $-\text{CH}_2-\text{O}-\text{P}$  group. Meanwhile, the chemical shifts at 39 and 48 ppm can be regarded as the two carbons in the  $-\text{CH}_2-\text{CH}_2$  groups in the IFR agent.

#### Elemental analysis

Elemental analytical results of the intermediate II and the IFR agent are listed in Table III. They agree well with the chemical formula:  $\text{NH}_2\text{CH}_2\text{CH}_2$  ( $\text{C}_5\text{N}_5\text{H}_7\text{O}$ ) $_2\text{H}$  and  $\text{C}_{17}\text{N}_{11}\text{H}_{31}\text{O}_{11}\text{P}_2$ .

#### Formulation and FR capabilities of the IFR/PU-based coatings

The addition of the IFR agent into PU varnish increases the LOI values from 17.3 for virgin PU to 34 for the 20% IFR/PU system.

Figure 7 shows the RHR data for PU and 20% IFR/PU systems from the cone calorimeter using a 50  $\text{kW}/\text{m}^2$  incident heat flux. The peak heat release rate was shown to be the most important parameter for predicting fire hazard. The presence of the IFR additives remarkably reduced the peak heat release rate compared with that of the virgin polymer. The RHR curve shows three maximal characteristic of a mate-

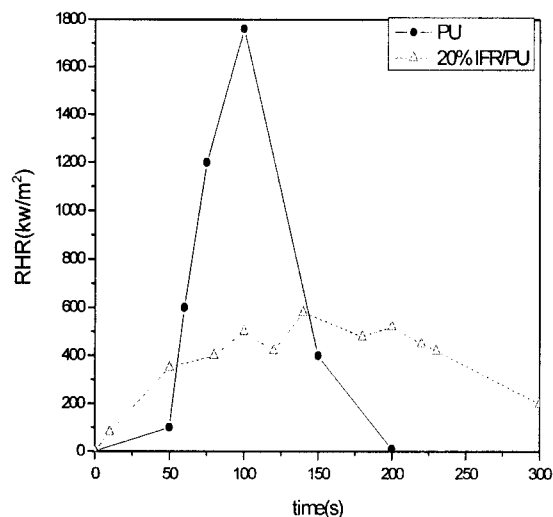


Figure 7 RHR values versus time for PU and 20% IFR/PU systems.

rial, typical of an intumescent system. After ignition, there is a rapid material degradation and, as a consequence, an increase of RHR. Then, the expanded protection shield forms and decreases RHR, given that material degradation is slowed down. At this time, there is a competition between material degradation and formation of the protective shield. Finally, an increase of the RHR indicates the intumescent shield degradation, which leads to the loss of the protective properties, although an expanded residue is present after extinction.<sup>16,23</sup>

The values of THE are shown in Figure 8. A comparison of the curves shows that the incorporation of the additive systems delays the accumulation of energy. Comparison of RHR and THE curves shows the importance of a rapid formation of the intumescent protective material to obtain good fire-retardant properties for the IFR/PU system.

In experimental conditions, the carbon monoxide (CO) and carbon dioxide ( $\text{CO}_2$ ) concentrations are high in the case of virgin PU attributed to a high degradation rate compared with that of the intumescent system (shown in Figs. 9 and 10).

The char index and weight losses of IFR/PU-coated woodblocks together with pure PU-coated woodblock are shown in Table IV.

As shown in Table IV, virgin PU-coated woodblock is more easily burned than the blank woodblock, attributed to the low resistance of PU to combustion (the virgin PU's LOI is about 17.3).<sup>24</sup> With the addition of 20% IFR agent, the weight loss and char index decrease markedly. Because a char index of about 25  $\text{cm}^3$  or lower and weight loss less than 5 g are considered the first grade in FR capability for wood-coating applications, the woodblock coated with the 20% IFR/PU system is considered to show excellent fire

TABLE III  
Elemental Analytical Data of Intermediate II and IFR Agent

Compound	Experimental (calculated) %			
	C	N	H	O
$\text{NH}_2\text{CH}_2\text{CH}_2$ ( $\text{C}_5\text{N}_5\text{H}_7\text{O}$ ) $_2\text{H}$	38.99 (39.24)	40.52 (41.96)	6.73 (5.72)	13.76 (13.08)
$\text{C}_{17}\text{N}_{11}\text{H}_{31}\text{O}_{11}\text{P}_2$	32.29 (32.53)	23.92 (24.57)	4.45 (4.94)	



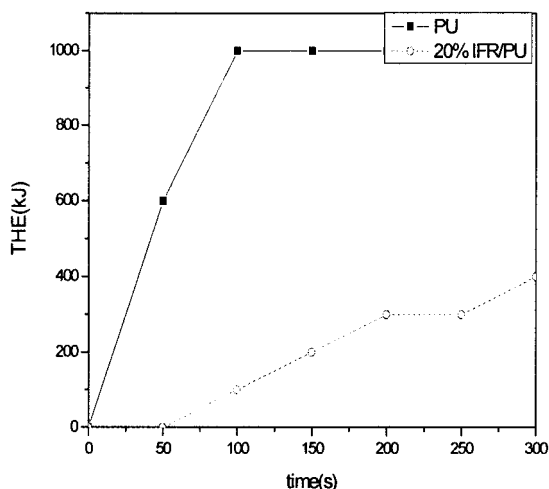


Figure 8 THE values versus time for PU and 20% IFR/PU systems.

retardancy.<sup>25,26</sup> In the next part of this study, this system was chosen to study other properties; that is, if not stated, the percentage of IFR agent in the IFR/PU system is 20%.

Figure 11 shows photographs and SEM micrographs of the burned surface of specimens prepared from pure PU-coated and IFR/PU-coated woodblocks. The two photographs show that in the case of PU-coated woodblock, the surface is relatively smooth compared with that obtained with IFR agent, which is characterized by agglomerates of swollen char. The SEM micrographs show an irregular swollen structure, in which pores of about 5–10 μm in diameter are recognizable in the char of the IFR/PU system, whereas the microstructure of char of the PU system is smooth. The many pores in the specimen obtained from the char of IFR/PU-coated woodblock can act as a physical barrier, which prevents combustible gases

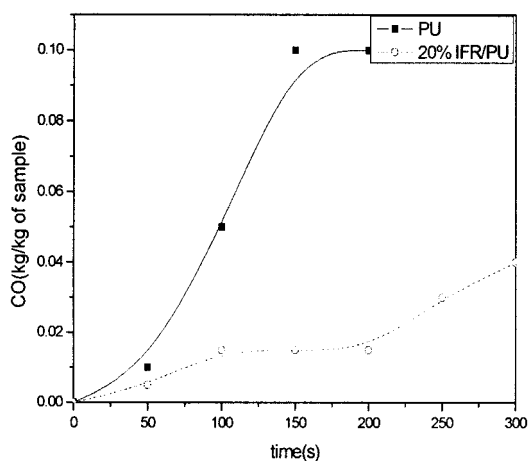


Figure 9 Total emission of CO for PU and 20% IFR/PU systems.

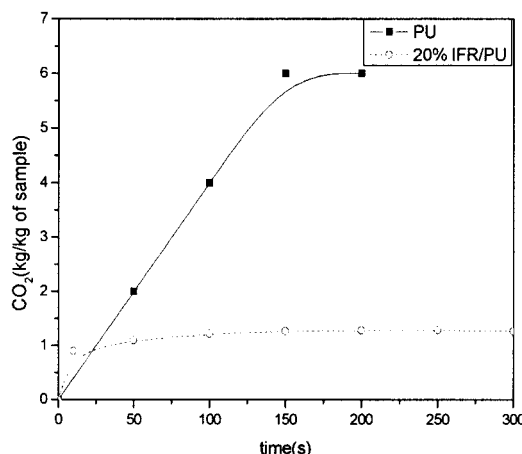


Figure 10 Total emission of CO<sub>2</sub> for PU and 20% IFR/PU systems.

from feeding the flame and also separates oxygen from the burning material.<sup>27,28</sup>

Thermal analysis

TGA curves of the IFR agent, PU, and IFR/PU are shown in Figure 12. Grassie and Scott<sup>29</sup> already reported the two degradation steps of PU. The first step starts from 220 to 400°C and the rate of weight loss is maximal at 320°C. The second step of degradation observed between 400 and 650°C leads to 0 wt % residue. The degradation of the IFR agent we synthesized also contains two steps. Between 320 and 450°C, the first step occurs; at higher temperature, the degradation continues and leaves a residue of about 10 wt %.

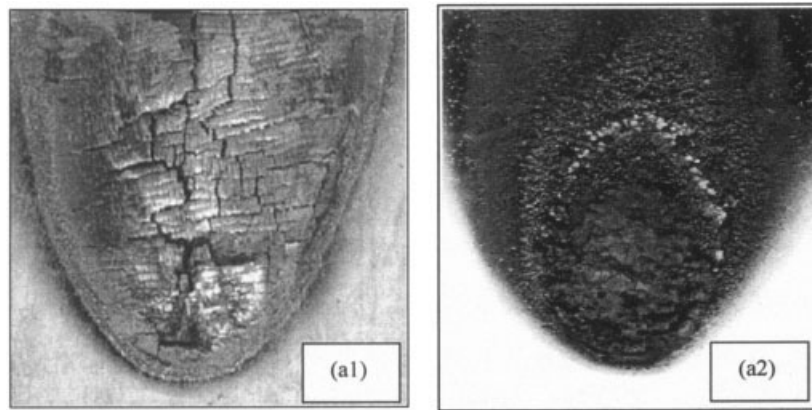
A TGA study of the IFR/PU system under air showed that the formulation of a carbonaceous material under air occurs in three successive steps. The first step, with a peak at about 300°C, may be assigned to the reaction between the IFR agent and PU. Then, the development of intumescent material occurs, followed by the formation of a carbonaceous material that is relatively stable in the temperature range 350–600°C; finally, the degradation of this material occurs with a stable residue of about 11%.

TABLE IV  
FR Test of Different Kinds of Coatings  
(Cabinet Method)

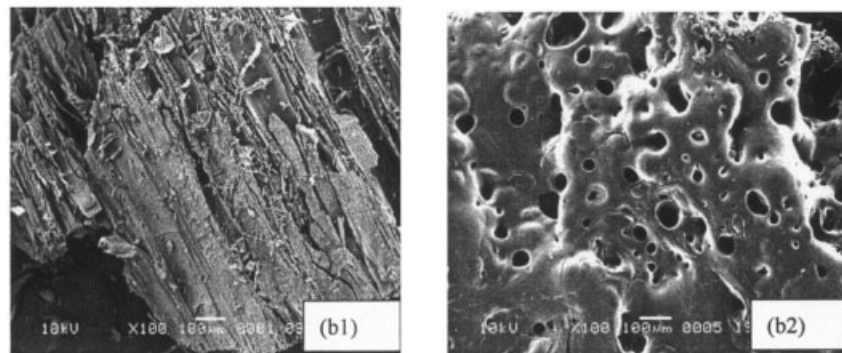
Sample	Weight loss <sup>a</sup> (g)	Char index <sup>b</sup> (cm <sup>3</sup> )
PU coating	89 ± 0.7	200 ± 1.4
IFR (20%)/PU-based coating	4.1 ± 0.3	5.5 ± 0.2

<sup>a</sup> Mean average weight loss of 5 unleached specimens.

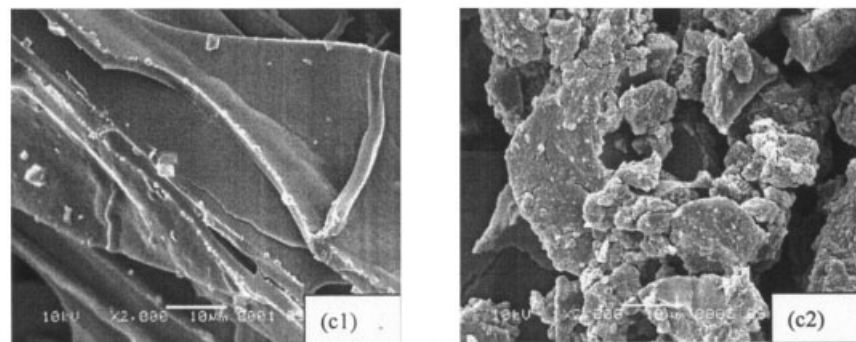
<sup>b</sup> Mean average char index of 5 unleached specimens.



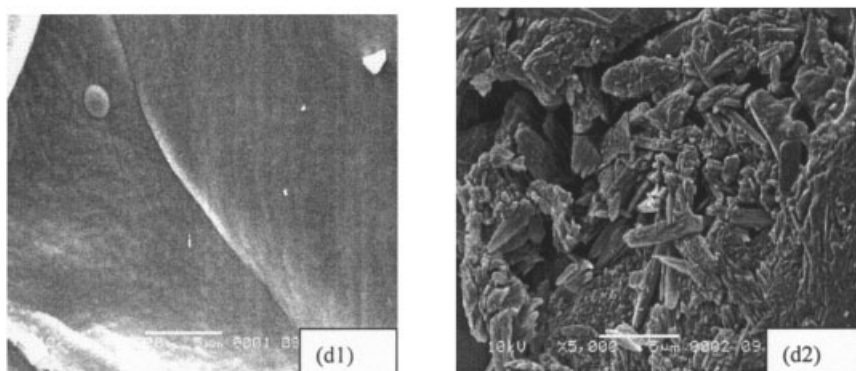
(c) Photographs of shape of different kinds of char  
 (a1) PU-coated woodblock; (a2) IFR/PU-coated woodblock



(d) SEM ( $\times 100$ ) of char surface (b1) PU; (b2) IFR/PU



(c) SEM ( $\times 2000$ ) of char surface (c1) PU; (c2) IFR/PU



(d) SEM ( $\times 5000$ ) of char surface (d1) PU; (d2) IFR/PU

**Figure 11** Photographs and SEM micrographs of char of PU and IFR/PU coating systems.

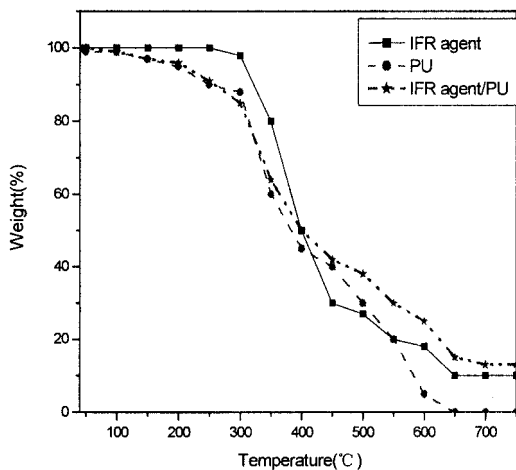


Figure 12 TGA curves of PU-based formulations.

A comparison between the experimental TGA curves of IFR/PU and the curves deduced from the linear combination of the TGA curves of the sole components is presented in Figure 13.<sup>30,32</sup> In the system, the weight difference curve is negative between 100 and 360°C under air, corresponding to the reaction between PU and IFR agent. It can be observed that a material relatively stable in the temperature range 360–600°C is formed. Consequently, it is obvious that the presence of the IFR agent in PU affects its thermal decomposition. In fact, the degradation products of the IFR agent, such as polyphosphoric compound, can react with PU and form a relatively more stable and a larger quantity of a high-temperature carbonaceous material. The degradation of the carbonaceous material in the 600–700°C then leads to formation of stable carbonaceous residues in the highest temperature range ( $T > 700^\circ\text{C}$ ).

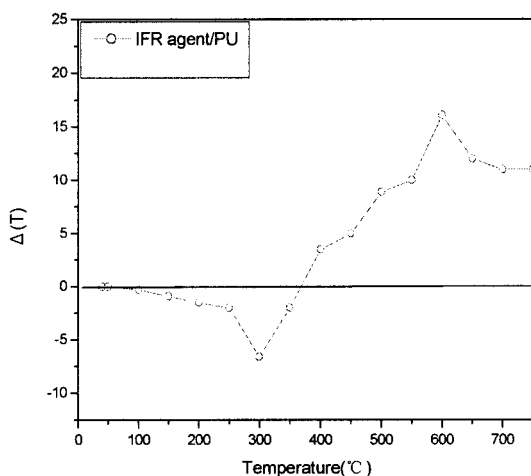


Figure 13  $\Delta(T)$  curves of IFR/PU system.

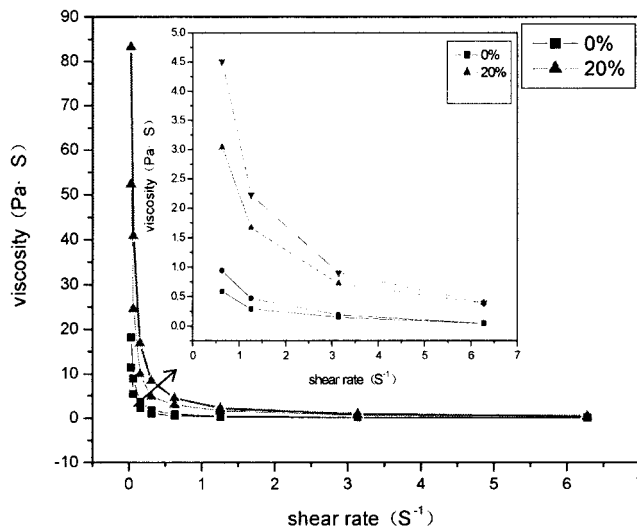


Figure 14 Viscosity–shear rate curves of PU and IFR/PU coating solutions.

**Rheology of IFR/PU-based coating solutions**

Figure 14 shows the variation of viscosity as a function of the shear rate in PU (0% IFR) and PU-based (20% IFR) coating solutions. The pure PU solution exhibits a slightly pseudoplastic behavior and a little thixotropy.<sup>13</sup> The presence of IFR additives in the coating solution produces an increase of pseudoplasticity and thixotropy. The pseudoplastic behavior indicates a rupture of the internal structure of the PU solution with shear, which additionally produces reversible changes between the “ordered” and “disordered” states, depending on the time. Moreover, the thixotropy property is also very important in coatings. It can make coatings appear to be solidlike or to be thick (high-viscosity) liquids at rest, but, when relatively small forces or deformations are applied to them (for example, gentle stirring or shaking), they become relatively mobile or low-viscosity liquids. When the force is removed, however, the structure may recover relatively quickly. A coating that exhibits thixotropy shows the following advantages: (1) it does not settle in the tin; (2) provided the recovery rate is not too low, it does not drop on vertical surfaces nor pull away from sharp edges; (3) heavier coats can be applied, thus economizing in labor.<sup>33</sup>

**Mechanical properties of dry IFR/PU-based coatings**

The mechanical properties of PU coatings with and without IFR additives are shown in Table V. It has already been established that the mechanical properties of PU can be affected by many factors including the chemical crosslinking level. Addition of IFR agent in the PU-based coating reduces the crosslink-

**TABLE V**  
**Mechanical Properties of IFR/PU-Based Coatings**

Sample	Crosslinking level	Hardness	Adhesion	Flexibility (mm)
PU coating	100%	H	0	0.5
IFR/PU-based coating	91%	2H	1	1.5

ing level, adhesion, and flexibility. This may be the result of the increased filler–polymer interactions in the system. In the IFR/PU system, the polymer chains, which firmly attach to the filler surface, may increase the internal stress within the polymer matrix, resulting in reduced adhesion to the substrate and flexibility as observed earlier.<sup>34</sup> Comparison of hardness of PU and IFR/PU-based coating systems shows that filler–polymer interaction may increase the overall rigidity of the matrix. This may be attributed to the filler possibly being located between

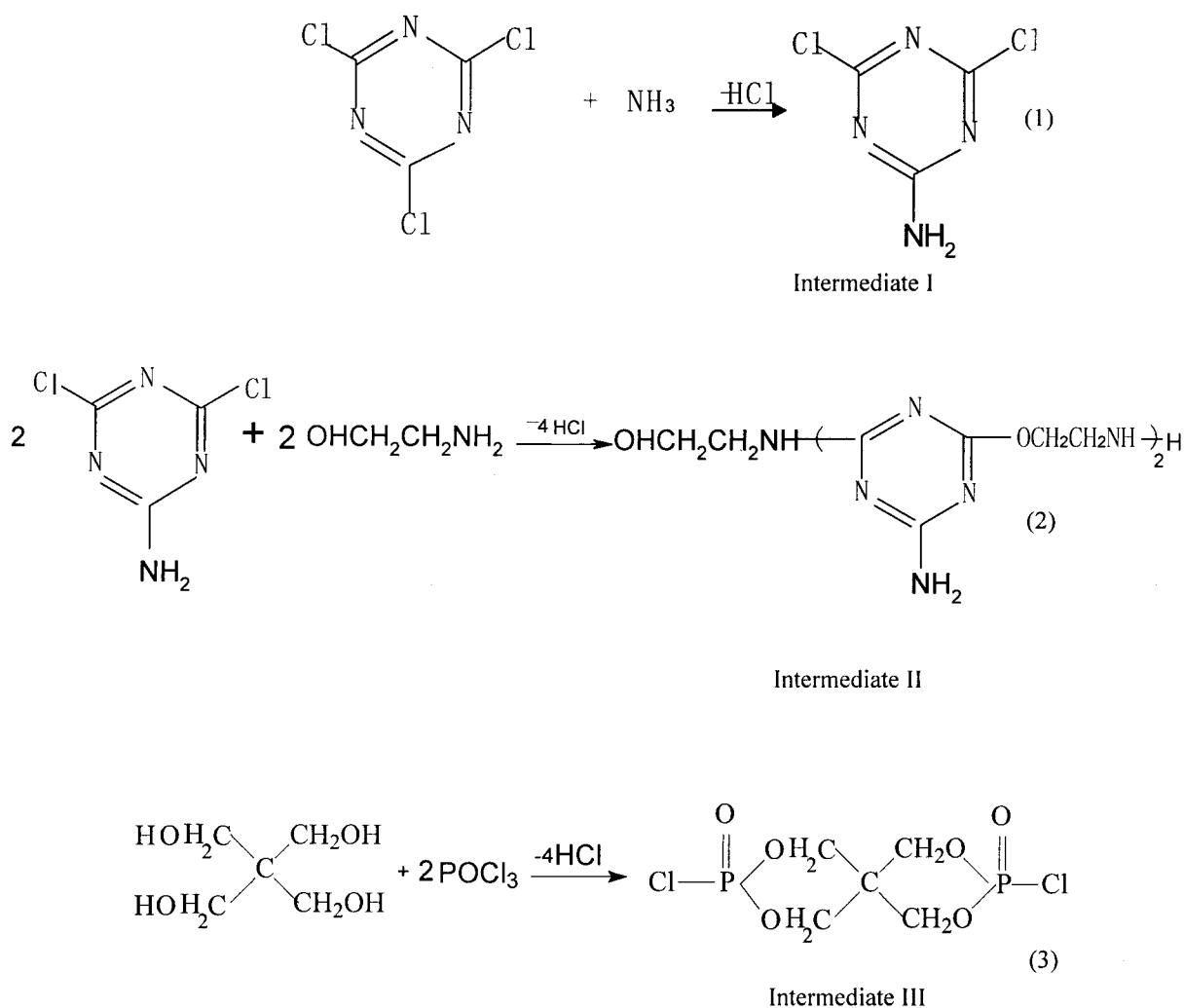
the PU chains like “crosslinking” points, reducing the distance of the chains in the structure and favoring crystallization of the PU chains at a lower degree of elongation.<sup>13</sup>

#### General remarks

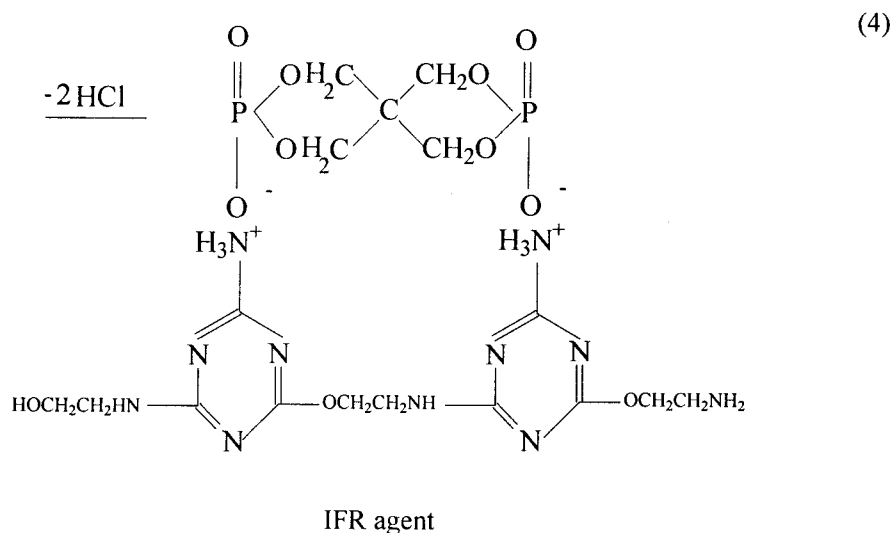
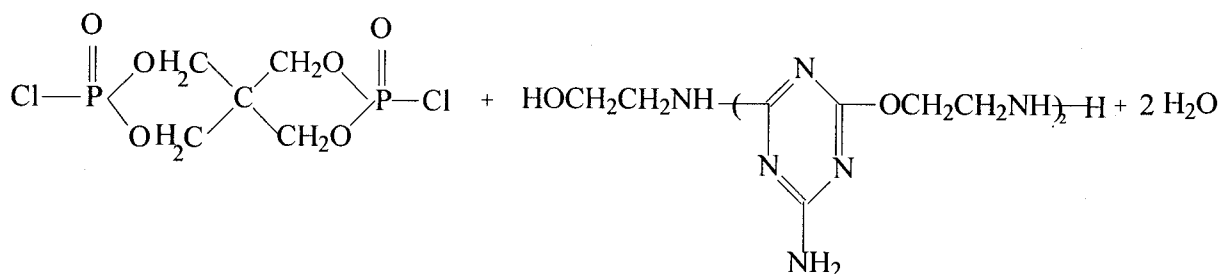
Regarding the FTIR, MAS-NMR <sup>13</sup>C, and elemental analysis results, we may conclude that the synthetic process may conform to following chemical equations as shown in **Scheme 1**. Containment of both P and N elements in the final structure favors the synergistic effect of fireproofing properties of the coating system.

It is evident that the pure PU has superior flammability, especially in a low LOI value, and high RHR, THE, CO, and CO<sub>2</sub> concentrations. By adding the IFR agent to the system, the RHR, THE, CO, and CO<sub>2</sub> concentrations decrease, and the LOI value is increased.

Addition of the IFR agent in PU can increase the hardness of the coating, but decrease the crosslinking



**Scheme 1a**



Scheme 1b

level of the system, and as a consequence, decrease the adhesion and flexibility of the coating.

### CONCLUSIONS

In this work, a novel IFR agent was synthesized and characterized by FTIR,  $^{13}\text{C}$ -NMR, and elemental analysis. The study of the FR properties of IFR/PU-based system by cone calorimeter clearly shows that the role the IFR agent plays in the system provides the desired fireproofing properties. Also, TGA and cabinet method analyses demonstrated that the IFR/PU system has excellent thermal stability. The photographs and SEM micrographs of intumescent char show that a physical barrier was developed during the fire-retardancy process. Moreover, the crosslinking level, hardness, adhesion, and flexibility show that this IFR/PU system has excellent mechanical properties.

The authors acknowledge the laboratory of East China University of Science and Engineering, Shanghai, China for help in the experiment and the "unknown" referee for very useful comments.

### References

- Kuryla, W. C.; Papa A. J. *Flame Retardancy of Polymeric Materials*; Marcel Dekker: New York, 1975; pp. 1, 3.
- Duquesne, S.; Le Bras, M.; Bourbigot, S. *J Appl Polym Sci* 2001, 82, 3262.
- Woods, G. *The I.C.I. Polyurethane Book*; ICI Polyurethanes and Wiley: Chichester, UK, 1990.
- Hatat, D. *Techniques de l'ingenieur*; Les Techniques de l'ingenieur: Paris, 1995.
- Kirk, R. E.; Othman D. F. *Encyclopedia of Chemical Technology*; Wiley-Interscience: New York, 1997.
- Melchior, M.; Sonntag, M.; Kobusch, C. *Prog Org Coat* 2000, 40, 99.
- Le Bras, M.; Bugajny, M.; Lefebvre, J. *Polym Int* 2000, 49, 1115.
- Bourbigot, S.; Le Bras, M.; Bugajny, M. In: *Proceedings of the NIST Annual Conference*, Gaithersburg, MD, 1998.
- Bourbigot, S.; Le Bras, M.; Delohel, R. *J Chem Soc Faraday Trans* 1996, 92, 149.
- Mamleev, V. Sh.; Gibov, K. M. *Fire Retardancy of Polymers: The Use of Intumescence*; The Royal Chemical Society: Cambridge, UK, 1998.
- Camino, G.; Costa, L.; Trossarelli, L. *Polym Degrad Stab* 1984, 6, 243.
- Ou, Y. X. *Jiangsu Chem Ind* 1998, 26, 6.
- Torro-Palau, A.; Fernandez-Garcia, J.; Orgiles-Barcelo, A. *J Adhes Sci Technol* 1997, 11, 247.
- Morice, L.; Bourbigot, S.; Leroy, J. M. *J Fire Sci* 1997, 15, 358.
- Babraukas, V. *Fire Mater* 1984, 8, 81.
- Bugajny, M.; Le Bras, M.; Bourbigot, S.; Poutch, F.; Lefebvre, J. M. *J Fire Sci* 1999, 17, 494.
- Gan, C.; Du, Y.; Gao, Y.; Liu, D. *J Coat China* 2000, 4, 23.
- Katritzky, A. R. *Physical Methods in Heterocyclic Chemistry*; Academic Press: New York/London, 1963.
- West, W. *Chemical Applications of Spectroscopy*; Rochester Eastman Kodak: New York, 1956.

20. Wang, Z.; He, X.; Sun, D. *Useful Analysis of Infrared Spectrum of Polymers*; Petroleum Industry Publication: Beijing, 1982.
21. Wang, J.; Yang, S.; Li, G.; Jiang, J. *J Fire Sci*, to appear.
22. Ning, Y. *Structural Identification of Organic Compounds and Organic Spectroscopy*; Science Publication: Beijing, 2000.
23. Bugajny, M.; Bourbigot, S.; Le Bras, M.; Delobel, R. *Polym Int* 1999, 48, 264.
24. Zhan, F.; Li, Y. *Functional Coatings*; Chemical Industry Publication: Beijing, 1988.
25. Chen-Yang, Y. W.; Chuang, J. R.; Yang, Y. C.; Chiu, Y. S. *J Appl Polym Sci* 1998, 69, 115.
26. GB 15442.1-1995. *Classification and test methods for fire retardancy of finishing fire retardant paints*. Beijing, China.
27. Bertelli, G.; Camino, G.; Marchetti, E.; Costa, L.; Locattli, R. *Angew Makromol Chem* 1989, 169, 137.
28. Bertelli, G.; Marchetti, E.; Camino, G.; Costa, L.; Locattli, R. *Angew Makromol Chem* 1990, 172, 156.
29. Grassie, N.; Scott, G. *Polymer Degradation and Stabilisation*; Cambridge University Press: Cambridge, UK, 1985.
30. Zhang, J.; Horrocks, A. R.; Hall, M. E. *Fire Mater* 1994, 18, 307.
31. Ye, L.; Cheng-pei, W.; Cai-yuan, P. *J Appl Polym Sci* 1998, 67, 2163.
32. Moric, L.; Bourbigot, S.; Leroy, J. M. *J Fire Sci* 1997, 15, 358.
33. Lamborne, R. *Paint and Surface Coatings: Theory and Practice*; Ellis Horwood: Chichester, UK, 1987.
34. Hegedus, C. R.; Kamel, I. L. *J Coat Technol* 1993, 822, 37.